Journal of Visualized Experiments

Functional Assessment of Kinesin-7 CENP-E in Spermatocytes using in vivo Inhibition, Immunofluorescence and Flow Cytometry

--Manuscript Draft--

Article Type:	Invited Methods Article - JoVE Produced Video
Manuscript Number:	JoVE63271R2
Full Title:	Functional Assessment of Kinesin-7 CENP-E in Spermatocytes using in vivo Inhibition, Immunofluorescence and Flow Cytometry
Corresponding Author:	Zhen-Yu She Fujian Medical University Fuzhou, Fujian CHINA
Corresponding Author's Institution:	Fujian Medical University
Corresponding Author E-Mail:	zhenyushe@fjmu.edu.cn
Order of Authors:	Meng-Fei Xu
	Yu-Hao Yang
	Ya-Lan Wei
	Jing-Lian Zhang
	Xuan Lin
	Xiao-Yan Lin
	Hui Chen
	Zhen-Yu She
Additional Information:	
Question	**Response**
Please specify the section of the submitted manuscript.	Biology
Please indicate whether this article will be Standard Access or Open Access.	Standard Access ($1400)
Please indicate the **city, state/province, and country** where this article will be **filmed**. Please do not use abbreviations.	Fuzhou, Fujian, China.
Please confirm that you have read and agree to the terms and conditions of the author license agreement that applies below:	I agree to the Author License Agreement
Please confirm that you have read and agree to the terms and conditions of the video release that applies below:	I agree to the Video Release
Please provide any comments to the journal here.	No comment.

TITLE:

Functional Assessment of Kinesin-7 CENP-E in Spermatocytes using *In Vivo* Inhibition, Immunofluorescence and Flow Cytometry

AUTHORS AND AFFILIATIONS:

Meng-Fei Xu[1,2], Yu-Hao Yang[1,2], Ya-Lan Wei[3,4], Jing-Lian Zhang[1,2], Xuan Lin[1,2], Xiao-Yan Lin[1,2], Hui Chen[1,2], Zhen-Yu She[1,2,*]

[1]Department of Cell Biology and Genetics, The School of Basic Medical Sciences, Fujian Medical University, Fuzhou, Fujian, 350122, China.
[2]Key Laboratory of Stem Cell Engineering and Regenerative Medicine, Fujian Province University, Fuzhou, Fujian, 350122, China.
[3]Fujian Obstetrics and Gynecology Hospital, Fuzhou, Fujian, 350011, China.
[4]Medical Research Center, Fujian Maternity and Child Health Hospital, Affiliated Hospital of Fujian Medical University, Fuzhou, Fujian, 350001, China.

Email Addresses of co-authors:

Meng-Fei Xu	(xumengfei@fjmu.edu.cn)
Yu-Hao Yang	(yuhaoyang@fjmu.edu.cn)
Ya-Lan Wei	(yalanwei@126.com)
Jing-Lian Zhang	(jinglianzhang@fjmu.edu.cn)
Xuan Lin	(linxuan@fjmu.edu.cn)
Xiao-Yan Lin	(xiaoyanlin@fjmu.edu.cn)
Hui Chen	(huichen@fjmu.edu.cn)
Zhen-Yu She	(zhenyushe@fjmu.edu.cn)

Corresponding Author:

Zhen-Yu She	(zhenyushe@fjmu.edu.cn)

KEYWORDS:

kinesin, spermatocyte, meiosis, CENP-E, spindle, chromosome, microtubule

SUMMARY:

This article reports an *in vivo* inhibition of CENP-E through abdominal surgery and testicular injection of GSK923295, a valuable model for male meiotic division. Using the immunofluorescence, flow cytometry and transmission electron microscopy assays, we show that CENP-E inhibition results in chromosome misalignment and genome instability in mouse spermatocytes.

ABSTRACT:

In eukaryotes, meiosis is essential for genome stability and genetic diversity in sexual reproduction. Experimental analyses of spermatocytes in testes are critical for the investigations

of spindle assembly and chromosome segregation in male meiotic division. The mouse spermatocyte is an ideal model for mechanistic studies of meiosis, however, the effective methods for the analyses of spermatocytes are lacking. In this article, a practical and efficient method for the *in vivo* inhibition of kinesin-7 CENP-E in mouse spermatocytes is reported. A detailed procedure for testicular injection of a specific inhibitor GSK923295 through abdominal surgery in 3-week-old mice is presented. Furthermore, described here is a series of protocols for tissue collection and fixation, hematoxylin-eosin staining, immunofluorescence, flow cytometry and transmission electron microscopy. Here we present an *in vivo* inhibition model *via* abdominal surgery and testicular injection, that could be a powerful technique to study male meiosis. We also demonstrate that CENP-E inhibition results in chromosome misalignment and metaphase arrest in primary spermatocytes during meiosis I. Our *in vivo* inhibition method will facilitate mechanistic studies of meiosis, serve as a useful method for genetic modifications of male germ lines, and shed a light on future clinical applications.

INTRODUCTION:

Meiosis is one of the most important, highly rigid, evolutionary conserved events in eukaryotic organisms, and is essential for gametogenesis, sexual reproduction, genome integrity, and genetic diversity[1–3]. In mammals, the germ cells undergo two successive cell divisions, meiosis I and II, after a single round of DNA replication. Unlike sister chromatids in mitosis, duplicated homologous chromosomes pair up and segregate into two daughter cells during meiosis I[4,5]. In meiosis II, sister chromatids pull apart and segregate to form haploid gametes without DNA replication[6]. Mistakes in either of the two meiotic divisions, including spindle assembly defects and chromosome missegregation, can result in the loss of gametes, sterility or aneuploidy syndromes[7–9].

Accumulating studies have shown that kinesin family motors play a crucial role in the regulation of chromosome alignment and segregation, spindle assembly, cytokinesis, and cell cycle progression in both mitotic and meiotic cells[10–12]. Kinesin-7 CENP-E (Centromere protein E) is a plus-end-directed kinetochore motor required for chromosome congression, chromosome transport and alignment, and the regulation of spindle assembly checkpoint in mitosis[13–18]. During meiosis, CENP-E inhibition by the specific inhibitor GSK923295 leads to cell cycle arrest, chromosome misalignment, spindle disorganization, and genome instability in spermatogenic cells[19]. The localization patterns and dynamics of CENP-E at the centromeres of dividing spermatocytes indicate that CENP-E interacts with kinetochore proteins for the sequential assembly of centromeres during meiosis I[20,21]. In oocytes, CENP-E is required for chromosome alignment and the completion of meiosis I[13,22,23]. Antibodies or morpholino injection of CENP-E results in misaligned chromosomes, abnormal kinetochore orientation, and meiosis I arrest in both mouse and *Drosophila* oocytes[23]. Compared with the essential roles of CENP-E in mitosis, the functions and mechanisms of CENP-E in meiosis remain largely unknown. Detailed mechanisms of CENP-E in chromosome congression and genome stability in male meiotic cells remain to be clarified.

Spermatogenesis is a complex and long-lasting physiology process, involving sequential spermatogonia proliferation, meiosis and spermiogenesis. Therefore, the whole process is

extraordinarily difficult to be reproduced *in vitro* in mammals and other species[24,25]. It is impossible to induce spermatocytes differentiation after the pachytene stage *in vitro*. Studies on male meiotic divisions have been generally limited to experimental analyses of early meiotic prophase[25,26]. Despite many technological endeavors, including short-term culture of spermatocytes[27,28] and organ culture methods[25], there are few effective methods to study male meiotic division. Furthermore, genetic deletion of essential genes usually results in developmental arrest and embryonic lethality. For example, mouse embryos lacking *CENP-E* fail to implant and cannot develop past implantation[29], which is an obstacle in mechanistic studies of CENP-E in meiosis. Taken together, establishing a practical and feasible system to study male meiotic division can greatly promote the research field of meiosis.

The small cell-permeable inhibitor is a powerful tool to study kinesin motors in cell division and developmental processes. The allosteric inhibitor, GSK923295, specifically binds to CENP-E motor domain, blocks the release of ADP (adenosine diphosphate), and finally stabilizes the interactions between CENP-E and microtubules[30]. In this study, an *in vivo* inhibition mouse model is presented through abdominal surgery and testicular injection of GSK923295. CENP-E inhibition results in chromosome misalignment in metaphase I of primary spermatocytes. Furthermore, CENP-E inhibition leads to meiotic arrest of spermatocytes and the disruption of spermatogenesis. A series of protocols are described for the analyses of spermatocytes and can be applied to observe meiotic spindle microtubules, homologous chromosomes, and subcellular organelles in spermatocytes. Our *in vivo* inhibition method is an effective method for the studies of meiotic division and spermatogenesis.

PROTOCOL:

All animal experiments were reviewed and approved by the Animal Care and Use Committee at Fujian Medical University (Protocol number SYXK 2016-0007). All mouse experiments were performed in accordance with the relevant guidelines of the Care and Use of Laboratory Animals of the National Institutes of Health (NIH publications number 8023, revised 1978).

1. Construction of GSK923295-mediated CENP-E inhibition mouse models

1.1. Fast the mice. Do not feed food and water for 24 h before operation. Sterilize surgical instrument by 121 °C for 30 min. Irradiate the surgical ultra-clean workbench with ultraviolet light for 2 h. Weigh the 3-week-old male ICR (Institute of Cancer Research) mice used for the experiments and calculate the doses of anesthetic required.

1.2. Anesthetize mice by inhalation of 0.2% ether and ensure the mice are completely anesthetized after 2–3 min. Check for the depth of anesthesia of the mice through a combination of mouse corneal reflex, nociceptive reflex, respiration, as well as muscle tone. Confirm the mice are deeply anesthetized.

1.3. Tie up the mouse limbs and fix them on the wax tray. Place a drop of vet ointment on mouse eyes to prevent dryness while under anesthesia. Shave the abdominal hair of the mouse from the lower abdomen to the scrotum using an experimental animal razor.

1.4. Disinfect the ventral abdomen with 75% ethanol for three times. Open the abdominal cavity using a sterile scalpel and make a <5 mm opening.

1.5. Clamp the skin with sterile surgical clamps and pull the epididymal fat pad with sterile dissecting forceps to locate the testes using a sterile tweezers. Fix the testis with sterile forceps under a stereoscope, and slowly inject 10 µL of GSK923295 into seminiferous tubules at a final concentration of 10 µM using 10 µL of rheodyne[30]. For the construction of the control group, inject 10 µL of 1% DMSO (dimethyl sulfoxide)/PBS (phosphate buffered saline) solution.

NOTE: Store the GSK923295 solution at a concentration of 10 mM at -80 °C. Dissolve 0.1 µL of 10 mM GSK923295 into 100 µL of PBS solution to prepare the 10 µM of GSK923295 solution.

1.6. Gently push the testis back into the abdominal cavity with sterile surgical forceps. Suture the peritoneum and skin simultaneously with two to four stitches using the suture line with diameter of 0.1 mm. Disinfect the wound with 75% ethanol, and then disinfect the wound with an iodine-based scrub.

1.7. Label a 3 x 3 mm place on the back of the animal with 3% picric acid solution using a cotton swab after abdominal surgery, put the mouse back to the feeding cage and ensure a clean and pathogen-free environment with sufficient food and water.

1.8. Keep the environment in a sterile state through the filtered air, the sterilized food and water. Take care of the animal until it has regained sufficient consciousness to maintain sternal recumbency. Ensure the mouseis not returned to the company of other animals until fully recovered.

NOTE: The mice are given postoperative care, and appropriately give the wound local anesthesia using 0.5% lidocaine to reduce postoperative pain when necessary.

2. Hematoxylin-eosin (HE) staining and histopathology

2.1. Four days after abdominal surgery, anesthetize mice with 1% ether for 5 min and euthanize the mice by excessive inhalation of ether anesthesia. Use surgical scissors to open the scrotum and remove the testes with forceps. Collect mouse testes 4 days after GSK923295 injection and fix them in 30 mL of 10% formaldehyde solution at room temperature for 12 h.

2.2. For gradient dehydration, sequentially incubate the sample in 40 mL of 70% ethanol for 1 h, in 40 mL of 85% ethanol for 1 h, in 40 mL of 95% ethanol for 1 h, and in 40 mL of 100% ethanol for 1 h.

2.3. Incubate the sample in 40 mL of xylene for 40 min, and then in 40 mL of paraffin for 1 h at 65 °C. Place the tissues at the bottom of the embedding box. Add the melted paraffin into the embedding box. Cool the tissues for complete solidification at 4 °C for 6 h.

2.4. Fix the samples on the holder of the ultramicrotome, keep the angle between the samples and the knife surface at 5–10°, and adjust the slice thickness to 5 µm. Prepare the 5 µm thick sections using an ultramicrotome, spread the slides in a water bath at 40 °C, and dry the sections in a slide drier for 12 h at 37 °C.

2.5. Incubate the slides in 200 mL of xylene for 40 min, in 200 mL of 100% ethanol for 6 min, in 200 mL of 95% ethanol for 2 min, in 200 mL of 90% ethanol for 2 min, in 200 mL of 80% ethanol for 2 min, and in 200 mL of 70% ethanol for 2 min, respectively.

2.6. Rinse the slides in distilled water for 5 min and stain them with the Mayer's hematoxylin solution for 6 min at room temperature.

NOTE: Mayer's hematoxylin solution: 0.011 mol/L hematoxylin, 6.7% anhydrous ethanol, 0.646 mol/L aluminum potassium sulphate, and 0.003 mol/L sodium iodate.

2.7. Rinse the slides in running water for 5 min and incubate with distilled water for 2 min.

2.8. Incubate the slides in 1% ethanol hydrochloride for 3 s, and then rinse them in running water for 2 min.

2.9. Stain the sample with 1% eosin for 15 s, and then incubate them with 95% ethanol for 5 s, with 100% ethanol for 2 min, and in xylene for 40 min.

2.10. Seal the slides using 15 µL of neutral gum and the 24 x 50 mm coverslip.

3. Immunofluorescence and confocal microscopy

3.1. Collect the 5 µm thick paraffin sections of mouse testes for immunofluorescence. Incubate the slides in xylene for 40 min, in 100% ethanol for 6 min, in 95% ethanol for 2 min, in 90% ethanol for 2 min, in 80% ethanol for 2 min, and in 70% ethanol for 2 min. Rinse the slides in distilled water for 5 min, and rinse the slides with 0.01 M PBS for 5 min.

3.2. Place the slides in the antigen retrieval solution (0.01 M citrate buffer) and boil under high pressure using a pressure cooker for 4 min for antigen retrieval. Cool the slides naturally to room temperature. Rinse with distilled water for 5 min twice, and with PBS for 5 min.

NOTE: 0.01 M citrate buffer (pH 6.0): 2.1 mmol/L citric acid, 11.6 mmol/L trisodium citrate dihydrate.

3.3. Permeabilize cells by incubating the slides in 500 µL of 0.25% TritonX-100/PBS for 10 min. Rinse the slides with PBS for 5 min three times.

3.4. For antigen blocking, incubate the samples with 300 µL of 3% bovine serum albumin

(BSA)/PBST (0.1% Tween-20 in PBS) for 1 h. Incubate the samples with the primary antibodies in 3% BSA/PBST for 16 h at 4 °C. Put the slides in a humidified box to prevent the tissues from drying out. Rewarm the slides naturally to room temperature for 30 min.

3.5. Discard the primary antibody, and then rinse the slides in PBST for 5 min three times. Dilute secondary antibodies in 3% BSA/PBST. Incubate the samples with secondary antibodies for 1–2 h at 37 °C. Rinse the samples in PBST for 5 min five times.

3.6. Stain the nuclei with 50 µL of 4', 6-diamidino-2-phenylindole (DAPI) for 5 min at room temperature. Mount the coverslip with the anti-fade mounting medium, and seal the coverslip with nail polish.

3.7. Observe and record fluorescent signals in the slides using a fluorescent microscope equipped with a NA 40x/ 0.75 objective.

4. Flow cytometry

4.1. Collect mouse testes in 6 cm Petri dishes and cut the testes into 1 mm^3 pieces using surgical scissors.

4.2. Digest the testes using 1 mL of 1% collagenase in 1.5 mL centrifuge tube for 10 min at 37 °C, and then centrifuge the samples at 1,000 x *g* for 5 min to precipitate spermatogenic cells.

4.3. Discard the supernatant, and then add 1 mL of 0.25% trypsin-EDTA (Ethylene Diamine Tetraacetic Acid) solution for 20 min at 37 °C, and then centrifuge the samples at 1,000 x *g* for 5 min.

4.4. Discard the supernatant, and then incubate the precipitated cells with 1 mL of 70% cold ethanol for more than 8 h at 4 °C.

4.5. Centrifuge the samples at 1,000 x *g* for 5 min, and then collect cell sediments. Stain the spermatogenic cells with 500 µL propidium iodide (PI) staining solution (50 µg/mL PI, 100 µg/mL RNase A and 0.2% Triton X-100 in PBS) at 37 °C for 30 min.

NOTE: Gently shake the centrifuge tube every 5 min to avoid cell aggregations.

4.6. Filter the samples using a 300 mesh screen to get rid of cell debris; collect the cells in a flow tube and store them at 4 °C.

4.7. Detect fluorescence signals and light scattering at the excitation wavelength of 488 nm using a flow cytometer. Analyze the DNA content and light scattering using the Modfit MFLT32 software.

5. Transmission electron microscopy

5.1. Cut the testes into 1 mm^3 pieces using the sharp scalpel, and quickly incubate the samples with 3% glutaraldehyde-1.5% paraformaldehyde solution in 0.1 M PBS (pH 7.2) for 4 h at 4 °C to avoid the changes of ultrastructure. Rinse the samples with 0.1 M PBS for 5 min three times.

NOTE: The scalpel and scissors should be sharp, and try to avoid artificial squeezing and pulling. The processing of samples should be carried out in the fixation fluid.

5.2. Fix the samples in 1% osmic acid-1.5% potassium ferrocyanide solution at 4 °C for 1.5 h. Dry the water with filter paper and rinse the samples with 0.1 M PBS for 5 min three times.

5.3. Dehydrate the samples in 40 mL of 50% ethanol for 10 min at 4 °C. Incubate the samples in 40 mL of 70% ethanol saturated uranium acetate dye at 4 °C for 12 h, in 40 mL of 90% ethanol for 10 min at 4 °C, in 40 mL of 90% ethanol-acetone for 10 min at room temperature, and in 40 mL of anhydrous acetone for 10 min three times at room temperature.

5.4. Incubate the samples in anhydrous acetone-epoxy resin 618 embedding agents (v / v = 1:1) mixture for 1.5 h, and then embedded the samples in epoxy resin 618 embedding agents at 35 °C for 3 h.

5.5. For resin polymerization, incubate the samples in epoxy resin 618 embedding agents at 35 °C for 12 h, at 45 °C for 12 h, and then at 60 °C for 24 h.

5.6. Install the samples and the glass knife, and then adjust the distances between the samples and the knife. Prepare the 90 nm thick ultra-thin sections using an ultra-thin microtome. Slice the samples at a constant speed, and then place the slides on a nickel mesh. Place the slides in a Petri dish at room temperature.

5.7. Stain the slides with 2% uranyl acetate for 10 min, and then stain the samples with 2% lead citrate for 10 min. Rinse the slides with distilled water. Dry the slides for 24 h at room temperature.

5.8. Observe the slides and record electron images at 70–100 kV using a transmission electron microscope.

REPRESENTATIVE RESULTS:

We have successfully constructed an *in vivo* CENP-E inhibition model of mouse testes through abdominal surgery and testicular injection of GSK923295[19]. The key technical steps of this method were shown in **Figure 1**. After testicular injection of GSK923295 for 4 days, the testes were harvested for further analyses. In the control group, the spermatogenic wave in the seminiferous tubules was regular and organized (**Figure 2A**). However, in the GSK923295 group, the spermatogenic wave were altered in the seminiferous tubules, and the metaphase arrested primary spermatocytes were significantly increased after CENP-E inhibition (**Figure 2B–D**). Importantly, several homologous chromosomes were not aligned at the equatorial plate after

CENP-E inhibition (**Figure 2B–D**). Furthermore, CENP-E inhibition also led to the increase of metaphase I spermatocytes in seminiferous tubules (**Figure 2E,F,G**). Taken together, CENP-E inhibition results in chromosome misalignment in primary spermatocytes during meiosis I, which suggests that CENP-E is responsible for chromosome congression and alignment of spermatocytes in meiosis.

To further validate these results, we performed the immunofluorescence assays to detect the spermatogenic cells in seminiferous tubules. We found that the regular spermatogenic wave shown in the control group was obviously changed and became irregular in the GSK923295 group (**Figure 3**). The meiotic spindle of dividing spermatocytes was labeled with anti-α-tubulin antibody, and the transverse filament of synaptonemal complexes in the spermatocytes was labeled with anti-synaptonemal complex protein 3 (SYCP3) antibody (**Figure 3A**). The SYCP3 positive cells per seminiferous tubule decreased after CENP-E inhibition (**Figure 3B**). Meanwhile, the SYCP3 dots per metaphase cell were not disrupted after CENP-E inhibition (**Figure 3C**). In addition, the SYCP3 stretches per cell were also not affected in the GSK92395 groups (**Figure 3D**). Strikingly, we found that the distances of spindle poles in metaphase I spermatocytes were increased after CENP-E inhibition (**Figure 3E,F**). These immunofluorescent results suggest that CENP-E is required for chromosome misalignment and the processes of spermatogenesis, and is indispensable for the maintenance of bipolar spindle and the organization of the meiotic spindle.

To investigate cell populations in mouse testes, we digested the testes and performed PI staining and flow cytometry assays (**Figure 4**). The important technical procedures were shown in **Figure 4A–C**. The spermatogenic cells consist of several cell populations, including the spermatogonia, primary spermatocytes, secondary spermatocytes, spermatids and spermatozoa. The DNA contents of these spermatogenic cells were shown in **Figure 4A**. We demonstrated that CENP-E inhibition resulted in the decrease of the haploid cells from 42.95 ± 1.09% in the control group to 38.26 ± 1.86% in the GSK923295 group (**Figure 4B–D**). The ratios of the diploid cells and aneuploidy cells were not significantly influenced after CENP-E inhibition (**Figure 4E,F**). Furthermore, the ratios of the tetraploid cells increase from 17.76 ± 1.52% in the control group to 28.88 ± 2.05% in the GSK923295 group (**Figure 4G**). Taken together, we find that cell populations of the spermatogenic cells are slightly altered after CENP-E inhibition. CENP-E inhibition results in the decrease of the haploid cells and the increase of tetraploid cells, which indicates that CENP-E inhibition is associated with metaphase arrest in the dividing spermatocytes.

Furthermore, we observed the submicroscopic structure of the spermatogenic cells using transmission electron microscopy (**Figure 5**). The chromatin organization, endoplasmic reticulum and mitochondria of spermatocytes were shown in **Figure 5**. We found that the organization of spermatogenic cells was slightly disrupted in the GSK923295 group (**Figure 5**).

FIGURE AND TABLE LEGENDS:

Figure 1: Establishment of an *in vivo* inhibition model of mouse testes through abdominal surgery and testicular administration. (**A**) All surgical instruments used in abdominal surgery. 1) dissecting scissor, 2) needle forceps, 3) straight forceps, 4) pincett, 5) rheodyne, 6) 1 mL syringe,

7) Scalpel with no. 3 handle and no. 11 blade, 8) stylolite, 9) round stitching needles, 1/2 0.6 x 14 mm, 1/2 0.7 x 17 mm, 10) ethanol swabs. (**B**) After anesthesia, the mice were placed in a supine position on a wax tray, the lower abdomen was prepared and disinfected with 75% ethanol. (**C**) A <5 mm opening was made in the middle of the lower abdomen. (**D**) The epididymal fat pad was pulled with sterile dissecting forceps to locate the testes. The testis was injected with 10 µL GSK923295 using a 10 µL rheodyne. (**E**) The peritoneum and skin was simultaneously sutured with two stitches. (**F**) The wound was disinfected with 75% ethanol.

Figure 2: CENP-E inhibition resulted in the arrest of meiosis I and chromosome misalignment in mouse spermatocytes. (**A**) HE staining of the spermatogenic cells in the control group. The arrows indicate the spermatocytes. (**B**) HE staining of the spermatogenic cells in the GSK923295 group. The testes were injected with GSK923295 for 4 days at a final concentration of 10 µM. The arrows indicate chromosome misalignment in the spermatocytes. For all images, scale bar, 10 µm. (**C**) Ratio of metaphase spermatocytes in seminiferous tubules. Control, 13.43 ± 1.68%; GSK923295, 42.29 ± 3.94%. N = 1308 cells were analyzed. Group = 4. Student's *t*-test. Error bars, means ± SEM. ***, $P < 0.001$. (**D**) Ratio of seminiferous tubules with dividing spermatocytes. Control, 5.38 ± 2.64%; GSK923295, 33.96 ± 3.87%. N = 151 seminiferous tubules were analyzed. Group = 4. (**E**) Immunofluorescence images of Histone H3 (phospho Ser 10) and TUBA4A in the control and GSK923295 groups. TUBA4A, red; Histone H3 (phospho Ser 10), green; DAPI, blue. Scale bar, 10 µm. The enlarged box is zoomed. (**F**) The quantification of the number of metaphase cells in seminiferous tubules. Control, 11.45 ± 1.55; GSK923295, 18.91 ± 2.36. N = 11. (**G,H**) Line-scan analyses of fluorescent intensities of Histone H3 and TUBA4A in metaphase I spermatocytes of the control group (**G**) and the GSK923295 group (**H**). TUBA4A, red; Histone H3 (phospho Ser 10), green; DAPI, blue. The X axis indicates the relative distance. The Y axis indicates fluorescent intensities. Student's *t*-test. Error bars, mean ± SEM. *, $P < 0.05$; ***, $P < 0.001$.

Figure 3: CENP-E inhibition by GSK923295 led to the disorganization of seminiferous tubules and the disruption of spermatogenesis. (**A**) Representative immunofluorescence images of SYCP3 and TUBA4A in the control and GSK923295 groups. SYCP3, red; TUBA4A, green; DAPI, blue. Scale bar, 10 µm. (**B**) Ratios of Histone H3 positive seminiferous tubules in the control and GSK923295 groups. Control, 56.00 ± 5.43%; GSK923295, 39.00 ± 1.73%. N = 10. (**C**) The quantifications of SYCP3 dots per metaphase cells. Control, 10.00 ± 1.02; GSK923295, 9.71 ± 0.86, N = 7. (**D**) The quantifications of SYCP3 stretches per cell in the control and GSK923295 groups. Control, 8.63 ± 0.22; GSK923295, 8.21 ± 0.21. N = 19. (**E**) The analyses of the distance of spindle poles in the metaphase I spermatocytes. Control, 8.20 ± 0.28 µm; GSK923295, 9.30 ± 0.29 µm. N = 30. (**F**) Immunofluorescence images of seminiferous tubules in the control and GSK923295 groups. The arrows indicate the spermatocytes. DAPI, green; β-tubulin, green. The enlarged images of the dashed box were shown in the zoom. For all images, scale bar, 10 µm. Student's *t*-test. Error bars, mean ± SEM. ns, $P > 0.05$; **, $P < 0.01$.

Figure 4: Flow cytometry analysis of spermatogenic cells in mouse testes. (**A**) Schematic illustrations of the key steps in cell cycle analysis of mouse spermatogenic cells. The diploid spermatocytes undergo meiosis I and II to form the haploid spermatids. The C value indicates the DNA content. The N value (ploidy) indicates the number of sets of chromosomes. (**B,C**) Flow

cytometry analysis of the spermatogenic cells in the control group (**B**) and the GSK923295 group (**C**). For *in vivo* CENP-E inhibition, GSK923295 was injected into 3-week-old male ICR mouse testes at a final concentration at 10 μM for 4 days. For cell cycle analysis, n = 3,000 cells were measured and analyzed. P4, the haploid cells (1C). P5, the diploid cells (2C). P6, the tetraploid cells (4C). (**D**) Ratios of the haploid cells in the control and GSK923295 groups. Control, 42.95 ± 1.09%; GSK923295, 38.26 ± 1.86%. N = 8. (**E**) Ratios of the diploid cells in the control and GSK923295 groups. Control, 20.10 ± 0.91%; GSK923295, 17.95 ± 0.81%. N = 8. (**F**) Ratios of the aneuploid cells (2C ~ 4C) in the control and GSK923295 groups. Control, 3.41 ± 0.23%; GSK923295, 3.39 ± 0.25%. N = 8. (**G**) Ratios of the tetraploid cells in the control and GSK923295 groups. Control, 17.76 ± 1.52%; GSK923295, 28.88 ± 2.05%. N = 8. For all graphs, Student's *t* test. Error bars, mean ± SEM. ns, $P > 0.05$; *, $P < 0.05$; ***, $P < 0.001$.

Figure 5: Electron microscopy analysis of the spermatogenic cells in the control and GSK923295 group. (**A**) Representative images of seminiferous tubules in the control group. Scale bar, 5 μm. (**B**) The enlarged image of the nucleus of the spermatocyte. The arrows indicate homologous chromatin of the spermatocytes. Scale bar, 1 μm. (**C**) The enlarged image of the cytoplasm of the spermatocytes. Scale bar, 1 μm. (**D**) Representative images of seminiferous tubules in the GSK923295 group. The testes were treated with 10 μM GSK923295 for 4 days. Scale bar, 5 μm. (**E**) The enlarged image of the nucleus of the spermatocyte in the GSK923295 group. Scale bar, 1 μm. (**F**) The enlarged image of the cytoplasm of the spermatocytes in the GSK923295 group. Scale bar, 1 μm. For all graphs, sc, spermatocyte; sd, spermatid. ER, endoplasmic reticulum; mt, mitochondria.

DISCUSSION:

In this study, we have established an *in vivo* CENP-E inhibition model of mouse testes using the abdominal surgery and microinjection of GSK923295. The abdominal surgery and testicular injection method used in this study has the following advantages. First, it is not limited to the age of mice. Experimenters can perform testicular injection at an early stage, for example, at 3-week-old or younger mice. Second, GSK923295 has a specific and excellent inhibitory effect on CENP-E. Third, this method is simple to operate and highly reproducible. In addition, the integrity of testes are maintained, which is suitable for the studies of intact tissues in the context of the organs.

There are several critical steps in this protocol. For example, it is important to maintain a sterile environment during abdominal surgery for the prevention of postoperative infections[31]. Furthermore, for mice of different ages or different experimental animals, the amounts of injection should be adjusted appropriately according to the size of the testes and the effectiveness of the drugs[19,32]. In addition, the proper digestion time and microscopic observation is required for the determination of single cells and subsequent cell population testing during flow cytometry. However, there are several limitations in this protocols. It is difficult to use abdominal surgery to construct a mouse model when the age of the mouse is less than 2 weeks old. The main reasons are that the mice are too young, the postoperative diet is difficult and the survival rate is low. The drugs used in animal models are liquid and have the characteristics of

easily penetrating cell membranes[19,32,33], which are suitable for the applications of this administration method.

Understanding meiosis is stimulated by *in vitro* cell culture and gene knockout studies, however, it is not easily applicable in mammalian spermatocytes[28]. The obstacle to the mechanistic studies of male meiosis has been the lack of an appropriate system for manipulation and observation of dividing spermatocytes in meiosis[27]. The mouse is an excellent model organism in the research of cellular and molecular mechanisms of meiosis during spermatogenesis. The first wave of mouse spermatocytes starts meiosis at day 10 post-partum (dpp) and develops into mature sperms at 35 dpp, which provides a developmental time-window for the studies of meiotic division and spermatogenesis[34].

Testis injection, including direct injection through the scrotum and microinjection *via* the abdominal surgery, is a useful technique for the studies of spermatogenesis[35,36]. Direct injection through the scrotum is quick and simple, and only causes a minor surgical trauma, which is suitable for mice of 4-week-old or older with the testes descend to the scrotum. However, it is impossible to inject the undescended testis of the 3-week-old or younger mice. Microinjection through the intraperitoneal surgery or scrotum surgery is suitable for the injection of undescended testes, which requires proficient surgical skills of experimental operators, a stereomicroscope, and the surgical and laboratory equipment. According to the injection sites, microinjection can be classified into seminiferous tubule injection, testicular net injection and testicular interstitial injection. Compared with other injection-based testis models, the injection of inhibitors through abdominal surgery can effectively inhibit the functions of proteins and have the advantages in cell membrane penetration, easy procedures, and long-term inhibition[19,32]. The methods using siRNAs, antisense oligonucleotides or lentivirus have greater limitations in low penetration efficiency of cell membranes, off-target side effects, and easy degradation of siRNA or oligonucleotides *in vivo*[37–40].

The meiotic division in living tissues is more complex than that in culture conditions, in which the tissue architecture, the developmental signaling and environmental factors *in vivo* should be taken into consideration[41]. Previous studies have demonstrated that culture media and cell autonomous factors are crucial for the stimulation of the onset of meiotic division phase. For example, the phosphatase inhibitor okadaic acid (OA)[42], spermatocyte-specific histone HIST1H1T[43], topoisomerase II[44], and metaphase promoting factor (MPF)[45] promote the G_2/MI transition in cultured spermatocytes. These complex culture conditions and factors contribute to the limitations of short-term culture of spermatocytes.

Direct injection of plasmid DNA into testes is successfully applied in testis mediated gene transfer and the production of transgenic mice[32,46]. The *in vivo* electroporation involves the injection of a DNA expression plasmid into the lumen of seminiferous tubules, and then use a series of electric pulses to change cell membrane permeability, improve the efficiency of transgene expression, and genetic modification[45–49]. Our method could be combined with *in vivo* electroporation, as well as fluorescent tagged proteins and gene editing tools, making this approach more powerful for the analyses of male meiotic division in the physiological context of tissues and organs.

ACKNOWLEDGMENTS:

We thank all members of the Cytoskeleton Laboratory at Fujian Medical University for helpful discussions. We thank Jun-Jin Lin at Public Technology Service Center, Fujian Medical University for technical assistances in flow cytometry. We thank Ming-Xia Wu and Lin-Ying Zhou at Electron Microscopy Lab of Public Technology Service Center, Fujian Medical University for technical assistances in electron microscopy. We thank Si-Yi Zheng, Ying Lin, Qi Ke, and Jun Song at Experimental Teaching Center of Basic Medical Sciences at Fujian Medical University for their supports. This study was supported by the following grants: National Natural Science Foundation of China (grant number 82001608), Natural Science Foundation of Fujian Province, China (grant number 2019J05071), Fujian Provincial Health Technology Project (grant number 2018-1-69), Startup Fund for Scientific Research, Fujian Medical University (grant number 2017XQ1001), Fujian Medical University high level talents scientific research start-up funding project (grant number XRCZX2017025) and Research project of online education and teaching of Chinese medicine graduate students (grant number B-YXC20200202-06).

DISCLOSURES:

The authors have nothing to disclose.

REFERENCES:

1. Lenormand, T., Engelstädter, J., Johnston, S. E., Wijnker, E., Haag, C. R. Evolutionary mysteries in meiosis. *Philosophical Transactions of the Royal Society of London. Series B, Biological Sciences*. **371** (1706), 20160001 (2016).
2. Brandeis, M. New-age ideas about age-old sex: separating meiosis from mating could solve a century-old conundrum. *Biological Reviews of the Cambridge Philosophical Society*. **93** (2), 801–810 (2018).
3. Lane, S., Kauppi, L. Meiotic spindle assembly checkpoint and aneuploidy in males versus females. *Cellular and Molecular Life Sciences: CMLS*. **76** (6), 1135–1150 (2019).
4. Handel, M. A., Schimenti, J. C. Genetics of mammalian meiosis: regulation, dynamics and impact on fertility. *Nature Reviews Genetics*. **11** (2), 124–136 (2010).
5. Miller, M. P., Amon, A., Ünal, E. Meiosis I: when chromosomes undergo extreme makeover. *Current Opinion in Cell Biology*. **25** (6), 687–696 (2013).
6. Duro, E., Marston, A. L. From equator to pole: splitting chromosomes in mitosis and meiosis. *Genes & Development*. **29** (2), 109–122 (2015).
7. Eaker, S., Pyle, A., Cobb, J., Handel, M. A. Evidence for meiotic spindle checkpoint from analysis of spermatocytes from Robertsonian-chromosome heterozygous mice. *Journal of Cell Science*. **114** (Pt 16), 2953–2965 (2001).
8. Faisal, I., Kauppi, L. Reduced MAD2 levels dampen the apoptotic response to non-exchange sex chromosomes and lead to sperm aneuploidy. *Development*. **144** (11), 1988–1996 (2017).
9. Bolcun-Filas, E., Handel, M. A. Meiosis: the chromosomal foundation of reproduction. *Biology of Reproduction*. **99** (1), 112–126 (2018).
10. Lawrence, C. J. et al. A standardized kinesin nomenclature. *The Journal of Cell Biology*. **167** (1), 19–22 (2004).
11. Cross, R. A., McAinsh, A. Prime movers: the mechanochemistry of mitotic kinesins. *Nature*

Reviews Molecular Cell Biology. **15** (4), 257–271 (2014).
12. Camlin, N. J., McLaughlin, E. A., Holt, J. E. Motoring through: the role of kinesin superfamily proteins in female meiosis. *Human Reproduction Update*. **23** (4), 409–420 (2017).
13. Yen, T. J., Li, G., Schaar, B. T., Szilak, I., Cleveland, D. W. CENP-E is a putative kinetochore motor that accumulates just before mitosis. *Nature*. **359** (6395), 536–539 (1992).
14. Wood, K. W., Sakowicz, R., Goldstein, L. S., Cleveland, D. W. CENP-E is a plus end-directed kinetochore motor required for metaphase chromosome alignment. *Cell*. **91** (3), 357–366 (1997).
15. Abrieu, A., Kahana, J. A., Wood, K. W., Cleveland, D. W. CENP-E as an essential component of the mitotic checkpoint in vitro. *Cell*. **102** (6), 817–826 (2000).
16. Mao, Y., Desai, A., Cleveland, D. W. Microtubule capture by CENP-E silences BubR1-dependent mitotic checkpoint signaling. *The Journal of Cell Biology*. **170** (6), 873–880 (2005).
17. Gudimchuk, N. et al. Kinetochore kinesin CENP-E is a processive bi-directional tracker of dynamic microtubule tips. *Nature Cell Biology*. **15** (9), 1079–1088 (2013).
18. Yu, K. W., Zhong, N., Xiao, Y., She, Z. Y. Mechanisms of kinesin-7 CENP-E in kinetochore-microtubule capture and chromosome alignment during cell division. *Biology of the Cell*. **111** (6), 143–160 (2019).
19. She, Z. Y. et al. Kinesin-7 CENP-E regulates chromosome alignment and genome stability of spermatogenic cells. *Cell Death Discovery*. **6**, 25 (2020).
20. Parra, M. T. et al. Sequential assembly of centromeric proteins in male mouse meiosis. PLoS Genetics. **5** (3), e1000417 (2009).
21. Parra, M. T. et al. Expression and behaviour of CENP-E at kinetochores during mouse spermatogenesis. *Chromosoma*. **111** (1), 53–61 (2002).
22. Duesbery, N. S. et al. CENP-E is an essential kinetochore motor in maturing oocytes and is masked during mos-dependent, cell cycle arrest at metaphase II. *Proceedings of the National Academy of Sciences of the United States of America*. **94** (17), 9165–9170 (1997).
23. Gui, L., Homer, H. Spindle assembly checkpoint signalling is uncoupled from chromosomal position in mouse oocytes. *Development*. **139** (11), 1941–1946 (2012).
24. Parks, J. E., Lee, D. R., Huang, S., Kaproth, M. T. Prospects for spermatogenesis in vitro. *Theriogenology*. **59** (1), 73–86 (2003).
25. Sato, T. et al. In vitro production of functional sperm in cultured neonatal mouse testes. *Nature*. **471** (7339), 504–507 (2011).
26. Staub, C. A century of research on mammalian male germ cell meiotic differentiation in vitro. *Journal of Andrology*. **22** (6), 911–926 (2001).
27. Handel, M. A., Caldwell, K. A., Wiltshire, T. Culture of pachytene spermatocytes for analysis of meiosis. *Developmental Genetics*. **16** (2), 128–139 (1995).
28. La Salle, S., Sun, F., Handel, M. A. Isolation and short-term culture of mouse spermatocytes for analysis of meiosis. *Methods in Molecular Biology*. **558**, 279–297 (2009).
29. Putkey, F. R. et al. Unstable kinetochore-microtubule capture and chromosomal instability following deletion of CENP-E. *Developmental Cell*. **3** (3), 351–365 (2002).
30. Wood, K. W. et al. Antitumor activity of an allosteric inhibitor of centromere-associated protein-E. *Proceedings of the National Academy of Sciences of the United States of America*. **107** (13), 5839–5844 (2010).
31. Nam, D., Sershon, R. A., Levine, B. R., Della Valle, C. J. The use of closed incision negative-

pressure wound therapy in orthopaedic surgery. *Journal of the American Academy Orthopaedic Surgeons*. **26** (9), 295–302 (2018).
32. She, Z. Y. et al. Kinesin-5 Eg5 is essential for spindle assembly and chromosome alignment of mouse spermatocytes. *Cell Division*. **15**, 6 (2020).
33. She, Z. Y. et al. Kinesin-6 family motor KIF20A regulates central spindle assembly and acrosome biogenesis in mouse spermatogenesis. *Biochimica et Biophysica Acta-Molecular Cell Research*. **1867** (4), 118636 (2020).
34. Wellard, S. R., Hopkins, J., Jordan, P. W. A seminiferous tubule squash technique for the cytological analysis of spermatogenesis using the mouse model. *Journal of Visualized Experiments: JoVE*. **132**, 56453 (2018).
35. Sato, M., Ishikawa, A., Kimura, M. Direct injection of foreign DNA into mouse testis as a possible in vivo gene transfer system via epididymal spermatozoa. *Molecular Reproduction and Development*. **61** (1), 49–56 (2002).
36. Coward, K. et al. Expression of a fluorescent recombinant form of sperm protein phospholipase C zeta in mouse epididymal sperm by in vivo gene transfer into the testis. *Fertility and Sterility*. **85**, 1281–1289 (2006).
37. Davis, S. et al. Potent inhibition of microRNA in vivo without degradation. *Nucleic Acids Research*. **37** (1), 70–77 (2009).
38. Zhao, H. T. et al. LRRK2 antisense oligonucleotides ameliorate α-Synuclein inclusion formation in a Parkinson's Disease mouse model. *Molecular Therapy-Nucleic Acids*. **8**, 508–519 (2017).
39. Shahzad, K. et al. CHOP-ASO Ameliorates Glomerular and Tubular Damage on Top of ACE Inhibition in Diabetic Kidney Disease. *Journal of the American Society of Nephrology*. **3**, ASN.2021040431 (2021).
40. Kang, K., Niu, B., Wu, C., Hua, J., Wu, J. The construction and application of lentiviral overexpression vector of goat miR-204 in testis. *Research in Veterinary Science*. **130**, 52–58 (2020).
41. Karabasheva, D., Smyth, J. T. Preparation of *Drosophila* larval and pupal testes for analysis of cell division in live, intact tissue. *Journal of Visualized Experiments: JoVE*. **159**, e60961 (2020).
42. Wiltshire, T., Park, C., Caldwell, K. A., Handel, M. A. Induced premature G2/M-phase transition in pachytene spermatocytes includes events unique to meiosis. *Developmental Biology*. **169** (2), 557–567 (1995).
43. Cobb, J., Cargile, B., Handel, M. A. Acquisition of competence to condense metaphase I chromosomes during spermatogenesis. *Developmental Biology*. **205** (1), 49–64 (1999).
44. Cobb, J., Reddy, R. K., Park, C., Handel, M. A. Analysis of expression and function of topoisomerase I and II during meiosis in male mice. *Molecular Reproduction and Development*. **46** (4), 489–498 (1997).
45. Inselman, A., Handel, M. A. Mitogen-activated protein kinase dynamics during the meiotic G2/MI transition of mouse spermatocytes. *Biology of Reproduction*. **71** (2), 570–578 (2004).
46. Muramatsu, T., Shibata, O., Ryoki, S., Ohmori, Y., Okumura, J. Foreign gene expression in the mouse testis by localized in vivo gene transfer. *Biochemical and Biophysical Research Communications*. **233** (1), 45–49 (1997).
47. Yamazaki, Y. et al. In vivo gene transfer to mouse spermatogenic cells by deoxyribonucleic acid injection into seminiferous tubules and subsequent electroporation. *Biology of Reproduction*. **59** (6), 1439–1444 (1998).

48. Yamazaki, Y., Yagi, T., Ozaki, T., Imoto, K. In vivo gene transfer to mouse spermatogenic cells using green fluorescent protein as a marker. *The Journal of Experimental Zoology*. **286** (2), 212–218 (2000).
49. Coward, K., Kubota, H., Parrington, J. In vivo gene transfer into testis and sperm: developments and future application. *Archives of Andrology*. **53** (4), 187–197 (2007).

Figure 1

Click here to access/download;Figure;Figure 1.tif

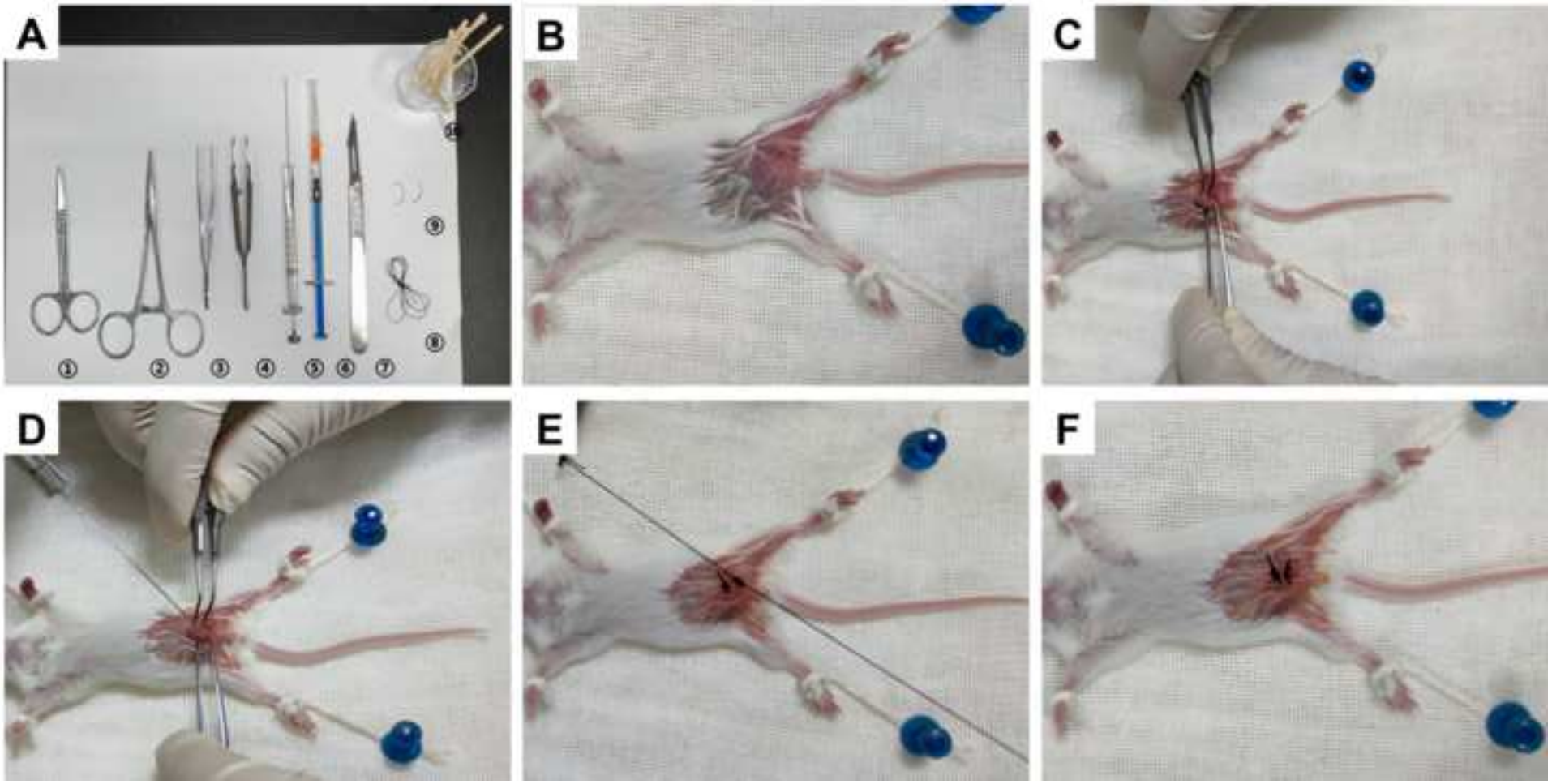

Figure 2

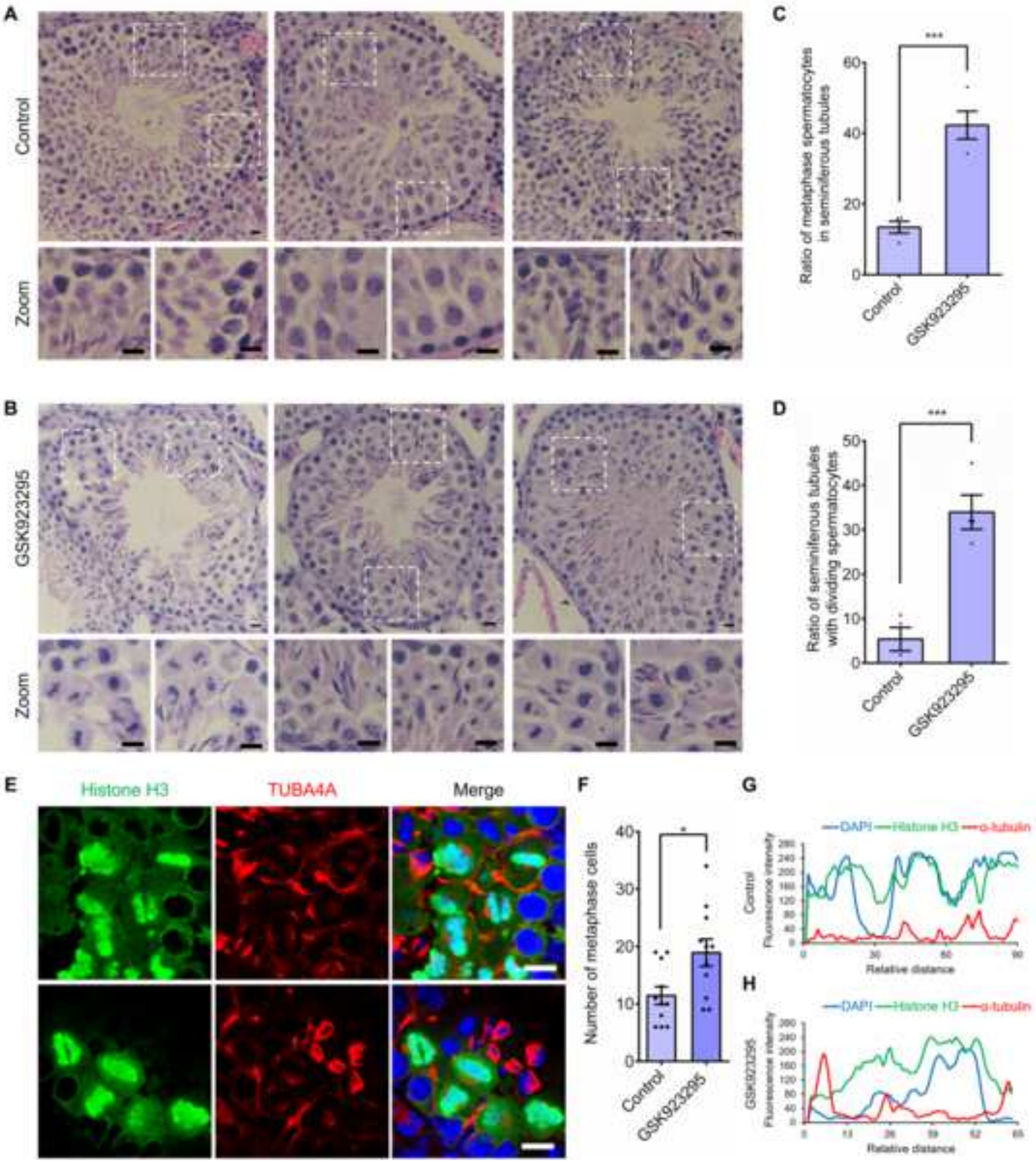

Figure 3

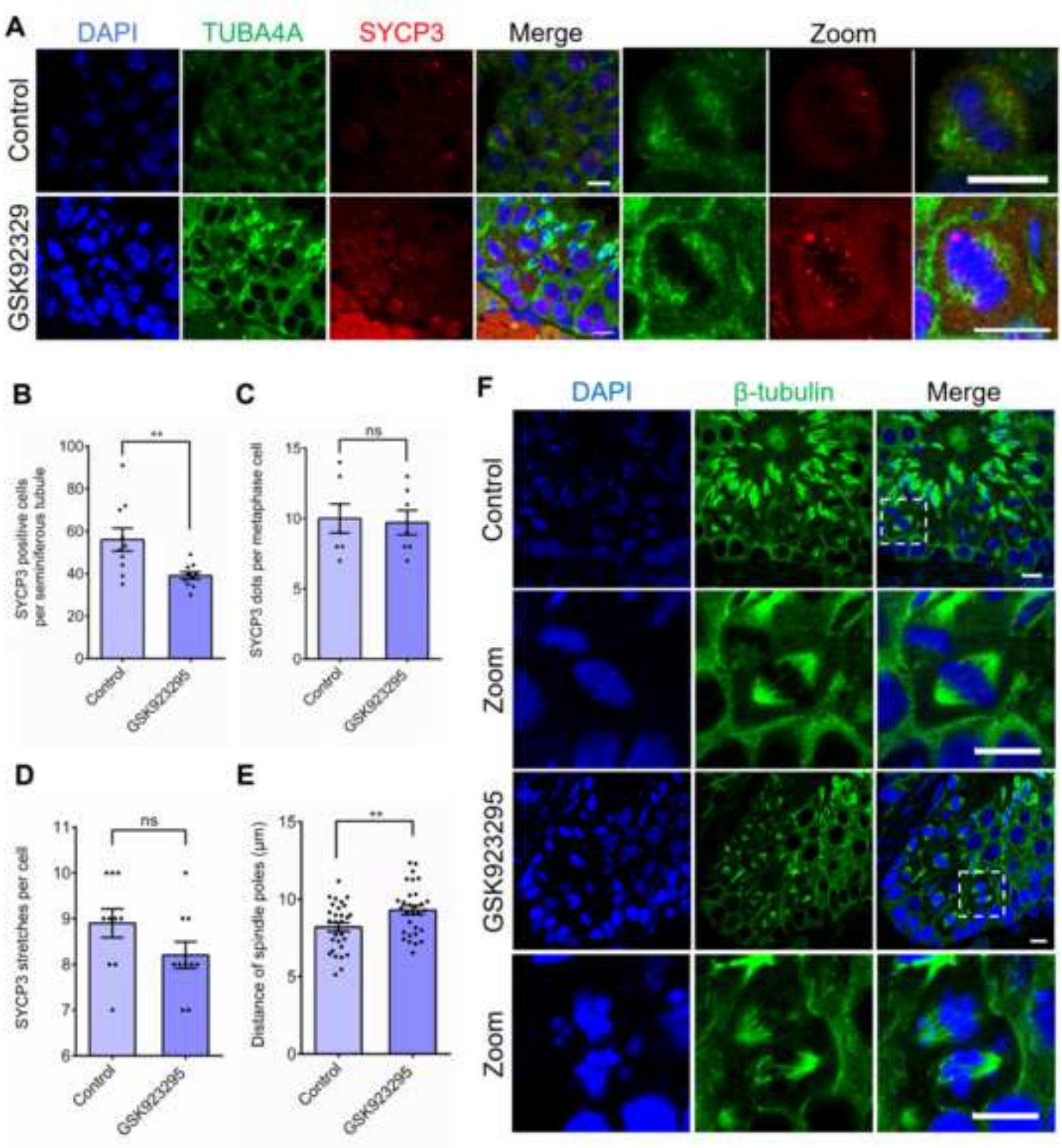

Figure 4

Click here to access/download;Figure;Figure 4.tif

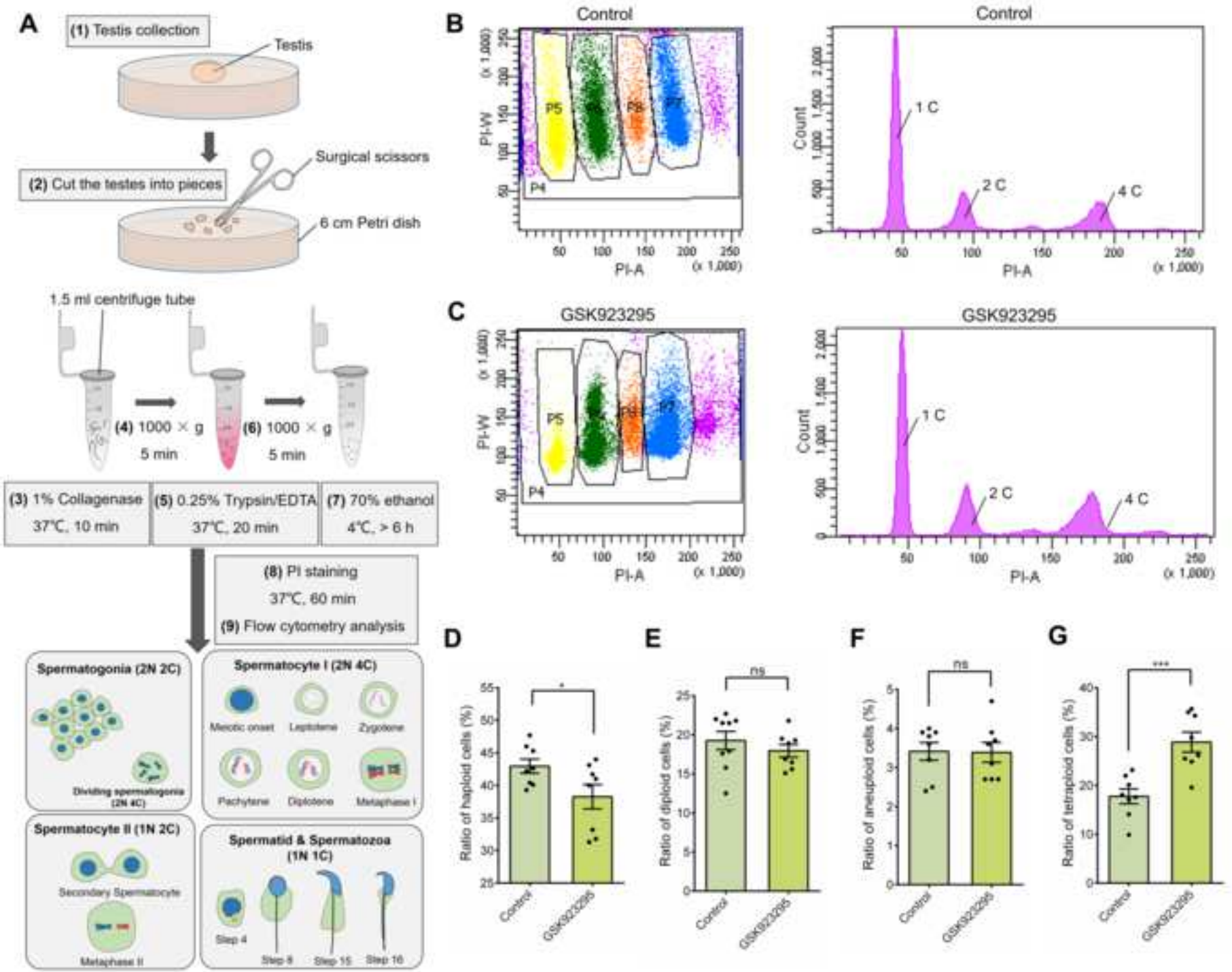

Figure 5

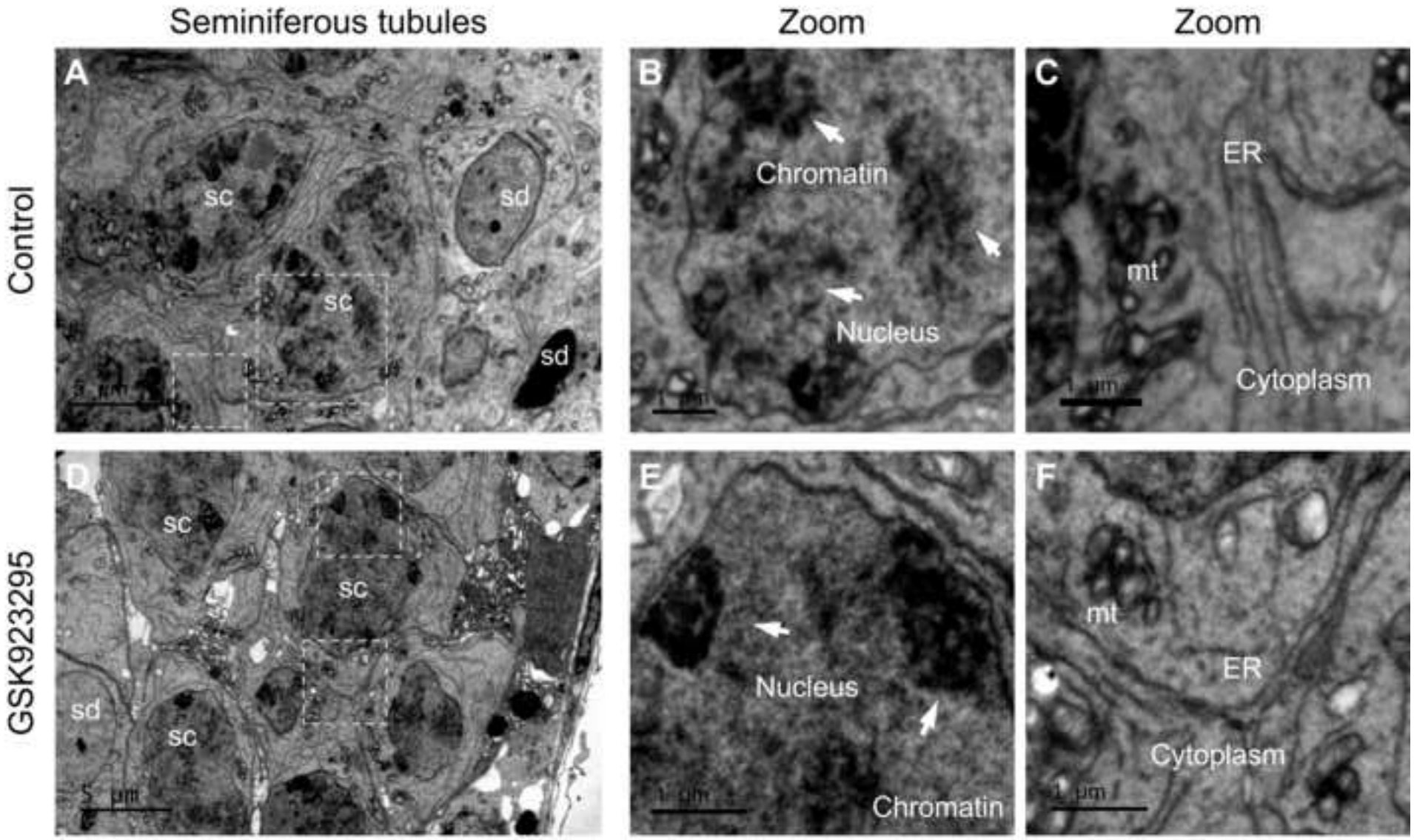

Click here to access/download
Table of Materials
material sheet.xlsx

Rebuttal Letter R2

22thNovember, 2021

Dear Editor Vineeta Bajaj,

Thank you very much for handling our manuscript JoVE63271R1 "Functional Assessment of Kinesin-7 CENP-E in Spermatocytes using in vivo Inhibition, Immunofluorescence and Flow Cytometry". We now submit a revised version of this manuscript R2 for further consideration (JoVE63271R2). We have carefully addressed all the comments and revised our manuscript accordingly to the comments. Now, we submit a rebuttal letter R2, and a revised version of the manuscript R2 to your journal.

We have addressed all editorial comments. We sincerely thank the editors and reviewers for their valuable comments. We agree with all these comments. We have carefully modified the manuscript and revised the figures accordingly. The point-by-point responses are listed under the comments in manuscript R2. The modifications are indicated in blue color in revised manuscript R2. According to the editorial comments, we have highlighted a 3 pages of the protocol section (highlight in yellow color) to be used for generating the script for the video.

Thank you very much. We are looking forward to your responses.

Best wishes,

Zhen-Yu She, Ph.D., Associate Professor

Fujian Medical University

E-mail: zhenyushe@fjmu.edu.cn

A List of Changes R2

Editorial comments:

1. The editor has formatted the manuscript to match the journal's style. Please retain and use the attached version for revision.

Answer: Thank you for your efforts. We have used the attached version for revision.

2. Please address specific comments marked in the manuscript.

Answer: Thank you for your valuable comments. We have addressed all the comments in manuscript R2. The response to each comment is listed under the comment. The modifications are indicated in blue color in revised manuscript R2.

3. Please proofread the manuscript well.

Answer: Thank you for your comments. We agree. We have carefully proofread and revised our manuscript accordingly. The modifications can be seen in blue color in revised manuscript R2 and also in A list of changes R2.

4. Please highlight 3 pages or less of the Protocol (including headings and spacing) that identifies the essential steps of the protocol for the video, i.e., the steps that should be visualized to tell the most cohesive story of the Protocol.

Answer: Thank you for your comment. We agree. We have highlight 3 pages of the protocol in yellow color for the video.

5. Please provide higher resolution for figure 1. Please do not show the face of the animal and zoom into the surgical site.

Answer: Thank you for your comment. We have revised the figure 1 and provide a higher resolution figure. We did not show the face of the animal and zoom in the surgical site this time in revised figure 1. The modifications can be seen in revised figure 1.

Reviewers' comments:

Reviewer #1:

Manuscript Summary:

The revised version is much improved. I have no further comment.

Answer: Thank you very much for your comments.

Reviewer #2:

Authors have addressed my concerns.

Answer: Thank you very much for your comments.

Changes of grammar and phrase custom consistency

Line 24, we have added “,”;

Line 30, “essential” was changed into “critical”;

Line 35, we have added “a”;

Line 38-40, “We validate the in vivo inhibition model via abdominal surgery and testicular injection is feasible and effective, which could be a powerful technique in the studies in male meiosis. ” was changed into “We construct an in vivo inhibition model via abdominal surgery and testicular injection, which could be a powerful technique in the studies of male meiosis.”;

Line 44, we have deleted “will”;

Line 50-52, “Unlike mitosis, duplicated homologous chromosomes rather than sister chromatids pair up and segregate into two daughter cells during meiosis I.” was changed into “”;

Line 59, “centromere” was changed into “Centromere”;

Line 62, we have added “the”;

Line 64, “pattern” was changed into “patterns”;

Line 72, “are worthy” was changed into “remain”;

Line 77, “promote spermatogenesis” was changed into “It is impossible to induce spermatocytes differentiation after the pachytene stage *in vitro*.”;

Line 77-79, “Research in male meiotic divisions has been generally limited to experimental analysis of early meiotic prophase.” was changed into “It is impossible to induce spermatocytes differentiation after the pachytene stage in vitro. Studies in male meiotic divisions have been generally limited to experimental analyses of early meiotic prophase.”;

Line 82, we have deleted “the”;

Line 82, we have deleted “are”;

Line 89, “and” was changed into “,”;

Line 89, “that” was changed into “and”;

Line 95, “that” was changed into “which”;

Line 95, “for the observation of” was changed into “to observe”;

Line 118, “Preoperative skin preparation from the lower abdomen to the scrotum. Shave the abdominal hair of the mice using an experimental animal razor.” was changed into “Shave the abdominal hair of the mice from the lower abdomen to the scrotum using an experimental animal razor.”;

Line 121, “70%” was changed into “75%”;

Line 128, we have deleted “and subject to the surgical procedures”;

Line 134, “70%” was changed into “75%”;

Line 134-135, we have added “, and then disinfect the wound with iodine based scrub”;

Line 141, “1.7.1.” was changed into “1.8.”;

Line 152, “After 4 days of surgery,” was changed into “4 days after abdominal surgery”;

Line 162, “Place the soaked tissues at the bottom of the embedding box, add the melted paraffin, and then let it cool to complete solidification at 4 °C for 6 h.” was changed into “Place the tissues at the bottom of the embedding box. Add the melted paraffin into the embedding box. Cool the tissues for complete solidification at 4 °C for 6 h.”.

Line 167, “slides” was changed into “sections”;

Line 178, we have added “and”;

Line 236, we have changed “precipitates” into “precipitated cells”;

Line 307, “compelxes” was changed into “complexes”;

Line 317, “three main” was changed into “several”;

Line 325, we have added “the”;

Line 326, “groups” was changed into “group”;

Line 329, “indicate” was changed into “indicates that”;

Line 329, we have added “the”;

Line 332, “through” was changed into “using”;

Line 342, “B.” was changed into “(B)”;

Line 343, “70%” was changed into “75%”;

Line 346, “syringe” was changed into “rheodyne”;

Line 347, “70%” was changed into “75%”;

Line 372, we have added “%”;

Line 372, “quantification” was changed into “quantifications”;

Line 410, “intraperitoneal surgical” was changed into “abdominal surgery and”;

Line 421, “amount” was changed into “amounts”;

Line 426, we have added “when the age is”.